

PAPER • OPEN ACCESS

Experimental and theoretical thermodynamic studies in $\text{Ba}_2\text{MgReO}_6$ —the ground state in the context of Jahn-Teller effect

To cite this article: Jana Pásztorová *et al* 2023 *J. Phys.: Condens. Matter* **35** 245603

View the [article online](#) for updates and enhancements.

You may also like

- [The Influence of Weak Ionic Interactions on Electrode Reactions during Electrodeposition of Re-Ni Alloys](#)
O. Berkh, A. Khatchaturians, N. Eliaz et al.
- [Nematicity-enhanced superconductivity in systems with a non-Fermi liquid behavior](#)
Sharareh Sayyad, Motoharu Kitatani, Abolhassan Vaezi et al.
- [Communication—A Mechanistic Study on Electrodeposition of Rhenium from Acidic Solution of Ammonium Perrhenate](#)
Huazhen Cao, Dagan Chai, Liankui Wu et al.

Experimental and theoretical thermodynamic studies in $\text{Ba}_2\text{MgReO}_6$ —the ground state in the context of Jahn-Teller effect

Jana Pásztorová^{1,*} , Aria Mansouri Tehrani², Ivica Živković¹, Nicola A Spaldin²  and Henrik M Rønnow¹

¹ Laboratory for Quantum Magnetism, Institute of Physics, École Polytechnique Fédérale de Lausanne, CH-1015 Lausanne, Switzerland

² Department of Materials, ETH Zurich, CH-8093 Zurich, Switzerland

E-mail: pasztorovaj@gmail.com

Received 25 October 2022, revised 15 February 2023

Accepted for publication 21 March 2023

Published 31 March 2023



Abstract

We address the degeneracy of the ground state multiplet on the $5d^1 \text{Re}^{6+}$ ion in double perovskite $\text{Ba}_2\text{MgReO}_6$ using a combination of specific heat measurements and density functional calculations. For $\text{Ba}_2\text{MgReO}_6$, two different ground state multiplets have previously been proposed—a quartet (with degeneracy $N = 4$) (Hirai and Hiroi 2019 *J. Phys. Soc. Japan* **88** 064712) and a doublet ($N = 2$) (Marjerrison *et al* 2016 *Inorg. Chem.* **55** 10701). Here we employ two independent methods for the estimation of phonon contribution in heat capacity data to obtain the magnetic entropy S_{mag} , which reflects the degeneracy of the ground state multiplet N through $S_{\text{mag}} = R \ln N$. In both cases, we obtain that in the temperature range covering 2 to 120 K the released entropy is better described by $S_{\text{mag}} = R \ln 2$. The detailed nature of the ground state multiplet in $\text{Ba}_2\text{MgReO}_6$ remains an open question.

Keywords: $\text{Ba}_2\text{MgReO}_6$, ground state multiplet, entropy, DFT, phonons

(Some figures may appear in colour only in the online journal)

1. Introduction

In recent years there has been an increase in interest in materials which exhibit strong spin–orbit coupling (SOC) with both experimental and theoretical studies revealing exotic phases, such as spin-liquids [1, 2] or systems with multipolar orders [3–5]. Since the strength of SOC grows rapidly with increasing

atomic number Z , it is important in materials containing $5d$ ions, where the entanglement between spin and orbital degrees of freedom profoundly affects the low-energy excitation spectrum.

One such family of compounds comprises double perovskites containing $5d$ elements Ta, Re and Os with formally single electron occupying their d orbitals ($5d^1$). These have general chemical formula $A_2BB'O_6$, with the magnetic B' ion surrounded by six anions, creating a highly symmetric octahedron. The octahedral crystal electronic field (CEF) splits the five-fold degenerate d orbitals into characteristic e_g and t_{2g} orbital sets (see figure 1). Under the influence of SOC the three-fold degenerate t_{2g} set (with an effective orbital momentum $l_{\text{eff}} = -1$) is split further into a lower-lying quartet

* Author to whom any correspondence should be addressed.



Original Content from this work may be used under the terms of the [Creative Commons Attribution 4.0 licence](https://creativecommons.org/licenses/by/4.0/). Any further distribution of this work must maintain attribution to the author(s) and the title of the work, journal citation and DOI.

($j_{\text{eff}} = 3/2$) and a doublet ($j_{\text{eff}} = 1/2$) at higher energy. Up to this point, the single ion ground state multiplet is the quartet ($N = 4$) proposed in [6] paper. However, further investigation of some double perovskites $A_2BB'O_6$ showed the structural distortion from cubic to tetragonal unit cell and elongation or compression of the ideal $B'-O_6$ octahedron along c -axis [7, 8]. In theory, this is known as Jahn-Teller effect that leads to another splitting of ground quartet into two Kramer doublets, where $N = 2$, and which translates into $R\ln 2$ value of entropy.

The coupling between magnetic moments has been considered to arise from a *super*-superexchange mechanism, comprising both ferromagnetic (J_{FM}) and antiferromagnetic (J_{AFM}) type and leading to a long-range magnetic order at T_m [3]. Additionally, it has been suggested that $5d^1$ systems could allow investigation of higher-order multipoles due to their small dipole magnetic moments [3]. For an electronic quadrupolar interaction V that is large enough, the prediction of a quadrupolar order at $T_q > T_m$ has been made [3]. This causes a small lattice distortion from a perfect cubic environment.

Several $5d^1$ double perovskites have been previously investigated in this context. In $\text{Ba}_2\text{NaOsO}_6$, where the Os ion is in a formally $7+$ valence state, a long-range magnetic ordering has been found to occur around $T_m = 7$ K [9–12], preceded by a breaking of local point symmetry, indicated by the splitting of nuclear magnetic resonance (NMR) spectra below 12 K [11]. Specific heat studies revealed a sharp transition at T_m [12, 13] and a small, broad shoulder extending towards higher temperatures. Authors assigned this shoulder to the nematic (orthogonal paramagnetic) phase based on temperature derivative of specific heat data [12]. For $B = \text{Li}$ only a single transition has been observed [9, 10] and no detailed specific heat studies have been reported. In the rhenium family several compounds have been investigated, all with Re in a formally $6+$ valence state and the B site occupied by $2+$ ions. For $B = \text{Mg}$, T_m occurs at 18 K [6, 14], with a broad shoulder revealed in calorimetric data around 33 K. This shoulder has been associated with a cubic to tetragonal structural distortion and argued to indicate the quadrupolar order [7]. DFT calculations further demonstrated the ordering of the proposed charge quadrupoles and suggested an additional spin-canting dependent ordered charge quadrupolar component [15]. A similar sequence of features has been revealed in $\text{Ba}_2\text{ZnReO}_6$ ($T_m = 16$ K, $T_q = 23$ K) [16] and $\text{Ba}_2\text{CdReO}_6$ ($T_m = 4$ K, $T_q = 25$ K) [17], pointing to a universal behavior across the family. Additionally, charge quadrupoles have also been recently discussed in the more ionic vacancy-ordered $5d^1$ double perovskite halides such as in Cs_2TaCl_6 [18].

Coming back to earlier discussion about the ground state multiplet of $5d^1$ systems, when the measured specific heat is used to extract the magnetic entropy, it has been observed in several reports to amount to a value significantly lower than the expected $R\ln 4$ [13, 14, 16]. For $\text{Ba}_2\text{NaOsO}_6$ it has been suggested that the missing entropy should be recovered at higher temperatures [13], although the NMR spectra show that the local environment is not distorted above ~ 12 K [11]. In contrast, recent single crystal experiments on $\text{Ba}_2\text{MgReO}_6$ [6]

indicate a complete $R\ln 4$ recovery, with the magnetic entropy being released all the way up to 80 K, much higher than $T_q = 33$ K. Similarly to the case of $\text{Ba}_2\text{NaOsO}_6$, an ideal cubic environment has been found in high resolution synchrotron diffraction experiment at $T > T_q = 33$ K [7]. Thus, there still remains an open question of the relationship between the magnetic entropy, ordering and ground state in $5d^1$ double perovskites.

In this article we focus our attention on the phonon background in $\text{Ba}_2\text{MgReO}_6$, which is a crucial component for obtaining the magnetic specific heat. There are several ways to estimate the phonon contribution including analytical approaches, first-principle calculations and by measuring a nonmagnetic analog in which the magnetic ion has been replaced with a non magnetic one. Hirai and Hiroi [6] used an analytical approach and showed that the sum of two Debye functions could describe the data above 80 K, although, there was no further clarification for use of these two Debye temperatures (299 K and 796 K) in particular, nor was the optical contribution addressed through Einstein modes. In this work, we determine of the phonon contribution by comparing measurements on newly synthesized powders of $\text{Ba}_2\text{MgReO}_6$ and its nonmagnetic analog Ba_2MgWO_6 . We complement our measurements with density-functional calculations of the phonon density of states, from which we extract the phonon specific heat.

2. Methods

2.1. Experimental details

Polycrystalline samples of $\text{Ba}_2\text{MgReO}_6$ and Ba_2MgWO_6 were prepared by a standard solid-state method following published papers [19, 20]. For $\text{Ba}_2\text{MgReO}_6$, stoichiometric amounts of BaO, MgO and ReO_3 were mixed and ground in an agate mortar under a protective argon atmosphere in a glove box. The mixture was placed into silica tubes, evacuated and sealed. The tubes were annealed in a box furnace for 24 h at 900 °C and cooled at the furnace cooling rate. For Ba_2MgWO_6 , the polycrystalline powder was prepared by repeated annealing and intermediate grinding. Powders of BaCO_3 , MgO and WO_3 were mixed in 2:1:1 ratios and ground in an agate mortar. The mixture was compressed into the pellet and heated up to 850 °C for 24 h. The initial reaction was followed by two annealing cycles with intermediate grinding and compression into a new pellet. First annealing was done at 1150 °C for 20 h and the second one at 1150 °C for 12 h.

The chemical composition of the polycrystalline samples was determined by powder x-ray diffraction on a Panalytical Empyrean diffractometer equipped with a PIXcel-1D detector, Bragg-Brentano beam optics and utilizing a monochromated $\text{Cu K}\alpha_{1,2}$ source ($\lambda_1 = 1.5406$ Å) at 300 K. The refinements of all samples using the *HighScore Plus* software were consistent with previous reports on powder samples [19, 20].

Specific heat measurements were performed using the relaxation method in a commercial apparatus (PPMS, Quantum Design). All polycrystalline samples were

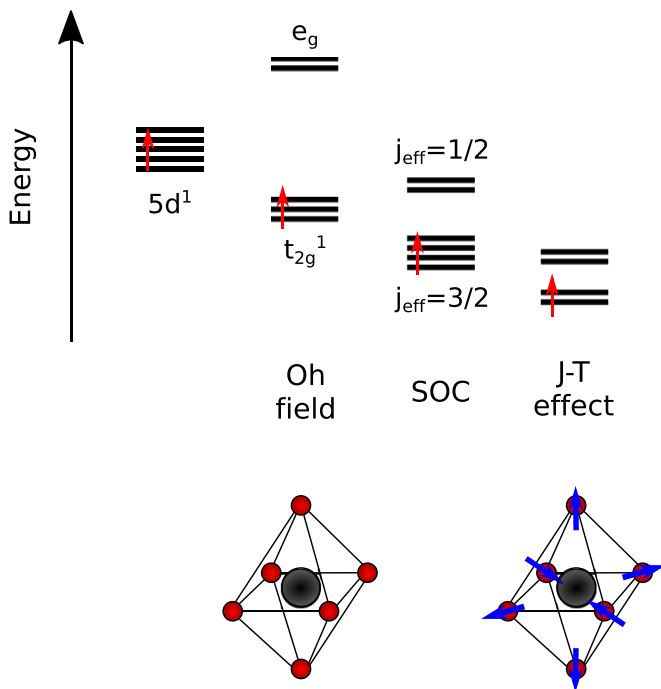


Figure 1. Proposed energy level splitting scheme for $5d^1$ electronic configuration in DPs (the splitting of higher energy levels is not shown for clarity). The final splitting of $j_{\text{eff}} = 3/2$ quartet into two doublets can be explained by Jahn-Teller (J)–(T) effect that is triggered by the distortion in the ideal Re-O₆ octahedron. The structural synchrotron data analysis [7] proved the existence of a phase transition from cubic to tetragonal space group at low temperatures. The displacement of oxygen ions is indicated by blue arrows.

compressed into pellets with diameter 3.2 mm, thickness under 0.5 mm and mass ~ 10 mg.

2.2. Computational details

Density functional theory (DFT) calculations were performed using a plane wave basis set and projected augmented wave potentials as implemented in the Vienna *ab-initio* simulation package (VASP) [21–24]. We used the following pseudopotentials: Ba_{sv} ($5s^2 5p^6 6s^2$), Mg_{pv} ($2p^6 3s^2$), Re_{pv} ($5p^6 5d^5 6s^2$), and O ($2s^2 2p^4$). The Perdew–Burke–Ernzerhof generalized gradient approximation was utilized to account for exchange and correlation, with an effective on-site Hubbard $U = 1.8$ eV correction applied to the d orbitals of the magnetic ions within the Dudarev scheme [25]. In addition, we included SOC using a full relativistic scheme [26]. An energy cutoff of 600 eV and a gamma-centered k -point mesh of $6 \times 6 \times 6$ were used. Electronic and structural optimizations were carried out with energy convergence criteria of 1×10^{-6} eV.

The crystal structure, including the internal atomic positions, was relaxed, while the experimental c/a ratio was constrained. The relaxed lattice parameters are $a = 5.8$ Å and $c = 8.2$ Å. As described in more detail in [15], the relaxed structure follows the qualitative distortions depicted in figure 1 with the distortion along the z -axis being smaller than the in-plane ones. Note that the unit cell possesses

two inequivalent Re sites with opposing distortions of their coordinating octahedra.

The magnetic structure, canted in-plane antiferromagnetism, was imposed as described in [15] by constraining the magnetic moments on the Re sites. The vibrational properties of Ba₂MgReO₆ were calculated using the open-source PHONOPY package [27], which constructs a force-constant matrix (calculated by VASP) by displacing symmetry-independent atoms by ± 0.01 Å from their equilibrium positions. Since DFT is a zero kelvin technique, phonon and therefore specific heat calculations are only calculated for the tetragonal ground-state crystal structure.

3. Experimental results

3.1. Phonon contribution to specific heat using the non-magnetic analogue

In figure 2(a) we present the measured specific heat of Ba₂MgReO₆ and Ba₂MgWO₆ powders. The Re compound exhibits two features reported in previous publications, a sharp peak at $T_m = 18$ K and a broad feature around $T_q = 33$ K. On the other hand the W compound displays a smooth behavior across the investigated range. As Ba₂MgReO₆ and Ba₂MgWO₆ are isostructural compounds, it is reasonable to expect similar phonon contribution of the specific heat as a function of temperature. In order to use the Ba₂MgWO₆ specific heat as estimate of the phonon specific heat in the Ba₂MgReO₆ compound, the W amplitude was scaled by a factor of 1.08 to match the high temperature part of the Re specific heat. There is also a small shift between the two curves along the temperature axis that is the result of different atomic masses of the two compounds, causing dissimilar characteristic Debye temperatures. We dismiss errors in heat capacity measurements that are lower than 0.5%. Minimal amount of low-temperature grease was used with negligible contribution to data inaccuracy.

We subtract this renormalized W curve from the Re data, presented in figure 2(b). The magnetic ordering at T_m and the broad bump around T_q are now emphasized, and the tail of the magnetic contribution can be seen to diminish above ~ 60 K. The magnetic entropy is then obtained by integrating $S_{\text{mag}} = \int (C_{\text{mag}}/T) dT$, and the result is presented in figure 2(c). The saturation value approaches 8 J K mol^{-1} , which is significantly lower than the expected $R \ln 4 = 11.5 \text{ J K mol}^{-1}$.

In figure 3 we plot the magnetic entropy as a function of temperature using different scaling factors for phonon part of specific heat to observe which values do not have physical meaning. The value of 1.08 is chosen in order to have the high temperature entropy approximately saturated, implying that the magnetic degrees of freedom are engaged only at low temperatures.

3.2. Phonon contribution to specific heat using first principles calculations

The calculated phonon specific heat is shown in figure 4(a), black circles, and presents similar temperature dependence as

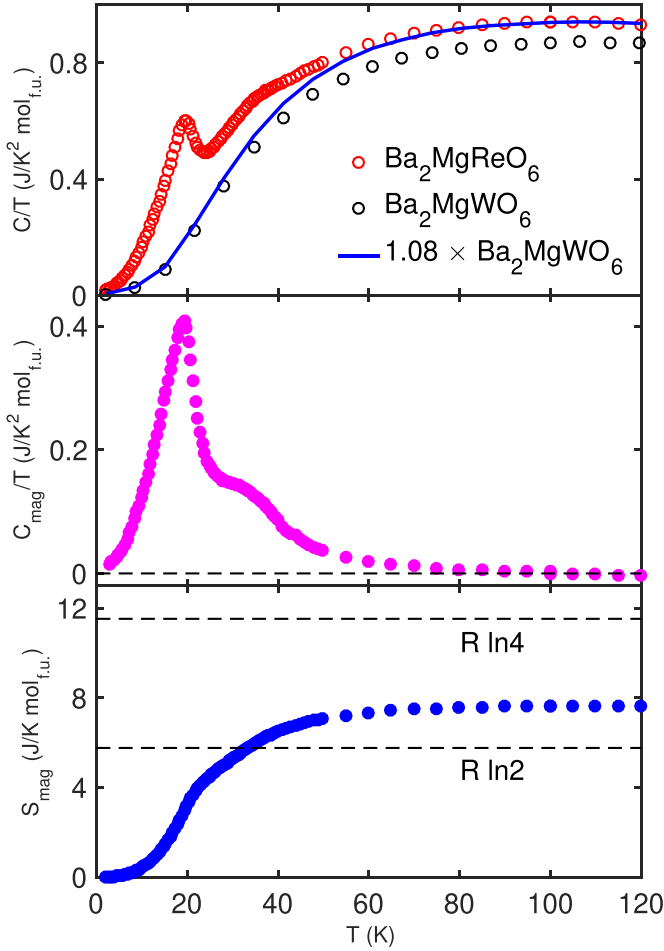


Figure 2. (a) Temperature dependence of specific heat divided by temperature C/T measured for $\text{Ba}_2\text{MgReO}_6$ powder ($5d^1$), red circles, and Ba_2MgWO_6 powder ($5d^0$), black circles. The solid blue line represents Ba_2MgWO_6 data scaled by 1.08. (b) Difference C_{mag}/T between magnetic and non-magnetic sample. (c) Entropy plot obtained from integrated C_{mag}/T for the $\text{Ba}_2\text{MgReO}_6$ powder.

data. As with the non-magnetic analog, we observe a slight mismatch between the maxima in C/T , in this case arising from two possible factors—one being an error in the calculation of interatomic forces and consequently the dynamic matrix, another is related to the approximation in phonon calculations (in case of DFT, the interatomic forces are calculated at zero kelvin and then phonons are elucidated using a harmonic approximation). Therefore we employ a renormalization factor to match the high temperature experimental data of $\text{Ba}_2\text{MgReO}_6$.

Figure 4(b) displays the subtraction of the experimental data and the calculated phonon background, revealing a similar shape as the C_{mag}/T in figure 2(b), with small differences above the magnetic transition—the non-magnetic analogue approach results in a slightly stronger T_q peak and a tail decaying slower towards high temperature. Above 50 K, the magnetic contribution C_{mag}/T oscillates very closely around $C_{\text{mag}}/T = 0$ value and start to increase slightly at 130 K meaning that the fit of high temperature data is not perfect (the

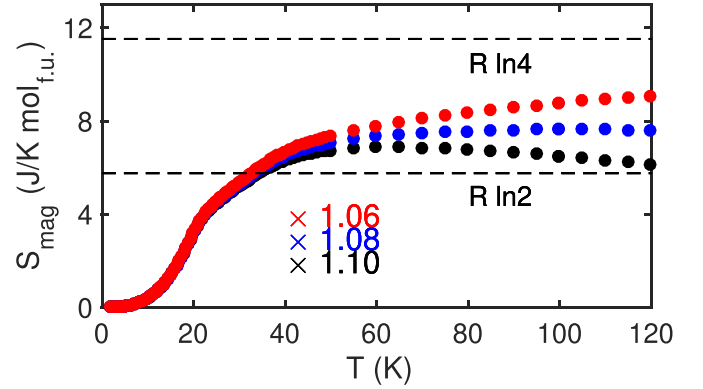


Figure 3. Entropy plot obtained from integrated C_{mag}/T using phonon background of non-magnetic Ba_2MgWO_6 studied in limits of different normalization factors—from 1.06 to 1.10. Negative slope or rapid increase of entropy in region above 60 K does not have physical meaning. The normalization factor of 1.08 was used as most suitable in figure 2.

deviation is less than 3% at 200 K). We attribute this mismatch to the discrepancies between C/T maxima of DFT and experimental data at higher temperatures. The resulting entropy in the range up to 120 K, figure 4(c), saturates above 50 K to a value within 95% of $R \ln 2$.

4. Discussion

The difference in extracted S_{mag} utilizing two methods in our work illustrates that the determination of the intrinsic phonon background of $\text{Ba}_2\text{MgReO}_6$ is not a straight forward process. Both the non-magnetic analog Ba_2MgWO_6 and the DFT calculations have their maximum in C/T slightly shifted towards higher temperatures compared to $\text{Ba}_2\text{MgReO}_6$. This results in an imperfect subtraction, causing C_{mag}/T values to oscillate around $C_{\text{mag}}/T = 0$ for temperatures above 120 K. Nevertheless, it is evident from the extracted results that the magnetic entropy up to ~ 120 K is significantly below the expected $R \ln 4$ for $N = 4$.

Our results are in general agreement with several other publications where magnetic entropy was extracted in $5d^1$ systems, covering both Os [13] and Re compounds [14, 28]. This indicates that the choice of the phonon background presented in [6] should not be regarded as a definitive proof of the total magnetic entropy reaching $R \ln 4$ above 2 K and that the missing entropy might be recovered at lower temperatures, within the ordered state. Previous suggestion [29] considered a possibility that a small distortion, below the detection level, keeps the doublet-doublet gap open to much higher temperatures. One should also take into account possible dynamical averaging of elongations along three equivalent directions which might get activated at higher temperatures. For those scenarios where the entropy might get released at substantially higher temperatures, specific heat is not reliable enough to confirm or refute them. Another point to make is the presence of a strong SOC for this family of compounds and structural distortions of ideal octahedron present in these compounds at T_q that might cause

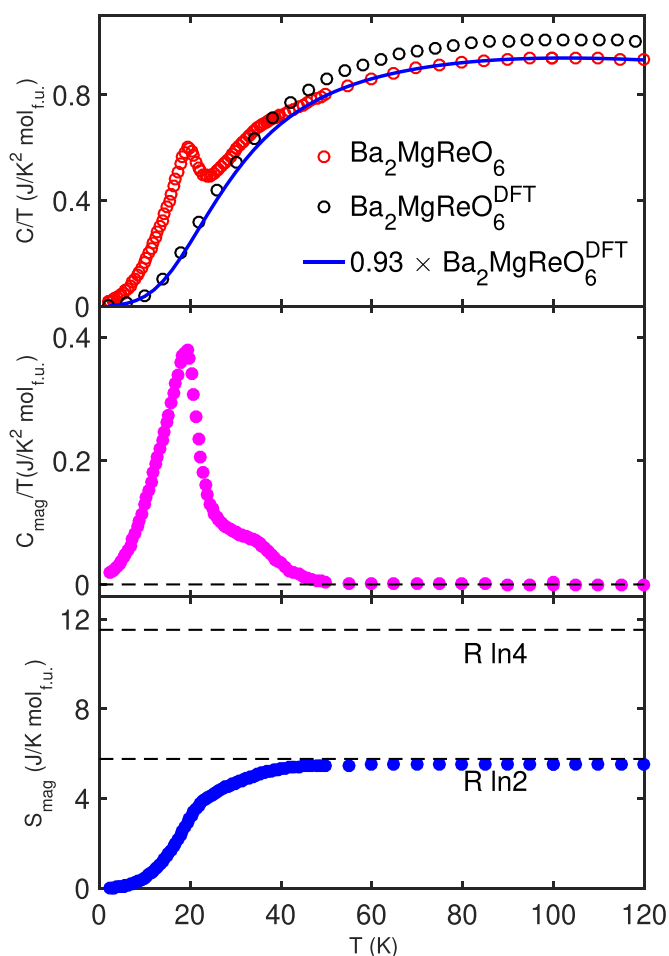


Figure 4. (a) Temperature dependence of specific heat divided by temperature C/T —experimental data for $\text{Ba}_2\text{MgReO}_6$ (red) and the phonon contribution for $\text{Ba}_2\text{MgReO}_6$ calculated from DFT (black). Solid blue line represents scaled DFT data. (b) C_{mag}/T shows the difference between experimental $\text{Ba}_2\text{MgReO}_6$ and DFT data. (c) Entropy plot obtained from integrating C_{mag}/T . The differences between two methods in figures 2 and 4 are very subtle—in case of non-magnetic analogue method, the second anomaly in C_m/T data is bigger and decreases to zero values slower.

further splitting of single ion ground state quartet into two Kramer doublets. As more $5d^1$ systems are emerging, it opens possibilities to study this ground state multiplet further, even employing more powerful experimental methods. The determination of the phonon part of heat capacity is non-trivial and require careful consideration.

5. Summary

We determined the phonon contribution to the heat capacity of $\text{Ba}_2\text{MgReO}_6$ by measuring its non-magnetic analog Ba_2MgWO_6 as well as calculating it from first principles. We find that both approaches give a slightly mismatched maximum in C/T , indicating a non-trivial problem of establishing phonon contribution at high temperatures. Both approaches result in total magnetic entropy reaching values significantly

lower than $R \ln 4$, which will hopefully instigate more detailed investigations to resolve this controversial issue.

Data availability statement

All data that support the findings of this study are included within the article (and any supplementary files).

Acknowledgments

This work was funded by the European Research Council (ERC) under the European Union's Horizon 2020 research and innovation program projects HERO (Grant No. 810451). Jana Pásztorová acknowledges support from the Federal Commission for Scholarships for Foreign Students for the Swiss Government Excellence Scholarship (ESKAS No. 2019.0041) for the academic year 2019-20.

ORCID iDs

Jana Pásztorová  <https://orcid.org/0000-0002-4762-0384>

Nicola A Spaldin  <https://orcid.org/0000-0003-0709-9499>

References

- [1] Krimmel A, Mucksch M, Tsurkan V, Koza M M, Mutka H and Loidl A 2005 *Phys. Rev. Lett.* **94** 237402
- [2] Wiebe C R, Greedan J E, Luke G M and Gardner J S 2002 *Phys. Rev. B* **65** 144413
- [3] Chen G, Pereira R and Balents L 2010 *Phys. Rev. B* **82** 174440
- [4] Chen G and Balents L 2011 *Phys. Rev. B* **84** 094420
- [5] Paramakanti A, Maharaj D D and Gaulin B D 2020 *Phys. Rev. B* **101** 054439
- [6] Hirai D and Hiroi Z 2019 *J. Phys. Soc. Japan* **88** 064712
- [7] Hirai D, Sagayama H, Gao S, Ohsumi H, Chen G, Arima T and Hiroi Z 2020 *Phys. Rev. Res.* **2** 022063
- [8] Ishikawa H, Takayama T, Kremer R K, Nuss J, Dinnebier R, Kitagawa K, Ishii K and Takagi H 2019 *Phys. Rev. B* **100** 045142
- [9] Stitzer K E, Smith M D and Zur Loye H-C 2002 *Solid State Sci.* **4** 311–6
- [10] Steele A J, Baker P J, Lancaster T, Pratt F L, Franke I, Ghannadzadeh S, Goddard P A, Hayes W, Prabhakaran D and Blundell S J 2011 Low-moment magnetism in the double perovskites Ba_2MnO_6 ($m = \text{Li, Na}$) *Phys. Rev. B* **84** 144416
- [11] Lu L, Song M, Liu W, Reyes A P, Kuhns P, Lee H O, Fisher I R and Mitrovic V F 2017 *Nat. Commun.* **8** 14407
- [12] Willa K, Willa R, Welp I R F U, Fisher I R, Rydh A, Kwok W-K and Islam Z 2019 *Phys. Rev. B* **100** 041108
- [13] Erickson A S, Misra S, Miller G J, Gupta R R, Schlesinger Z, Harrison W A, Kim J M and Fisher I R 2007 *Phys. Rev. Lett.* **99** 016404
- [14] Marjerrison C A et al 2016 *Inorg. Chem.* **55** 10701–13
- [15] Mansouri Tehrani A and Spaldin N A 2021 Untangling the structural, magnetic dipole and charge multipolar orders in $\text{Ba}_2\text{MgReO}_6$ *Phys. Rev. Mater.* **5** 104410
- [16] da Cruz Pinha Barbosa V et al 2022 The impact of structural distortions on the magnetism of double perovskites containing $5d^1$ transition-metal ions *Chem. Mater.* **34** 1098–109

- [17] Hirai D and Hiroi Z 2021 *J. Phys.: Condens. Matter* **33** 135603
- [18] Tehrani A M, Soh J-R, Pásztorová J, Merkel M E, I Živković, H M Rønnow and Spaldin N A 2023 Charge multipole correlations and order in Cs_2TaCl_6 *Phys. Rev. Res.* **5** L012010
- [19] Bugaris D E, Hodges J P, Huq A and Zur Loye H-C 2011 *J. Solid State Chem.* **184** 2293–8
- [20] Bramnik K G, Ehrenberg H, Dehn J K and Fuess H 2002 *Solid State Sci.* **5** 235–341
- [21] Kresse G and Hafner J 1993 *Ab initio* molecular dynamics for liquid metals *Phys. Rev. B* **47** 558–61
- [22] Kresse G and Furthmüller J 1996 Efficient iterative schemes for *ab initio* total-energy calculations using a plane-wave basis set *Phys. Rev. B* **54** 11169–86
- [23] Kresse G and Joubert D 1999 From ultrasoft pseudopotentials to the projector augmented-wave method *Phys. Rev. B* **59** 1758–75
- [24] Blöchl P E 1994 Projector augmented-wave method *Phys. Rev. B* **50** 17953–79
- [25] Dudarev S L, Botton G A, Savrasov S Y, Humphreys C J and Sutton A P 1998 Electron-energy-loss spectra and the structural stability of nickel oxide: AnLSDA+U study *Phys. Rev. B* **57** 1505–9
- [26] Steiner S, Khmelevskyi S, Marsmann M and Kresse G 2016 Calculation of the magnetic anisotropy with projected-augmented-wave methodology and the case study of disordered $\text{Fe}_{1-x}\text{Co}_x$ alloys *Phys. Rev. B* **93** 224425
- [27] Togo A and Tanaka I 2015 First principles phonon calculations in materials science *Scr. Mater.* **108** 1–5
- [28] Ishikawa H, Hirai D, Ikeda A, Gen M, Yajima T, Matsuo A, Matsuda Y H, Hiroi Z and Kindo K 2021 Phase transition in the $5d^1$ double perovskite $\text{Ba}_2\text{CaReO}_6$ induced by high magnetic field *Phys. Rev. B* **104** 174422
- [29] Lu L, Song M, Liu W, Reyes A P, Kuhns P, Lee H O, Fisher I R and Mitrović V F 2017 *Nat. Commun.* **8** 14407